Arylacetamide deacetylase attenuates fatty-acid-induced triacylglycerol accumulation in rat hepatoma cells

Vivien Lo,*,† Bruce Erickson,†,§ Michaela Thomason-Hughes,†,§ Kerry W. S. Ko,†,§ Vernon W. Dolinsky,§ Randy Nelson,† and Richard Lehner[1],*,†,§

Department of Cell Biology,* Department of Pediatrics,§ and the Group on the Molecular and Cell Biology of Lipids,† University of Alberta, Edmonton, Alberta T6G 2S2, Canada

Abstract Mobilization of hepatic triacylglycerol stores provides substrates for mitochondrial β-oxidation and assembly of VLDLs; however, the identity of lipolytic enzymes involved in the regulation of this process remains largely unknown. Arylacetamide deacetylase (AADA) shares homology with hormone-sensitive lipase and therefore could potentially participate in hepatic lipid metabolism, including the regulation of hepatic triacylglycerol levels. We have established McArdle-RH7777 (rat hepatoma) cell lines stably expressing mouse AADA cDNA and performed metabolic labeling as well as lipid mass analyses. Expression of AADA cDNA in McArdle-RH7777 cells significantly reduced intracellular triacylglycerol levels and apolipoprotein B secretion and increased fatty acid oxidation. These results suggest that fatty acids released by AADA-mediated hydrolysis of lipids are channeled for β-oxidation rather than for the assembly of lipoproteins.—Lo, V., B. Erickson, M. Thomason-Hughes, K. W. S. Ko, V. W. Dolinsky, R. Nelson, and R. Lehner. **Arylacetamide deacetylase attenuates fatty-acid-induced triacylglycerol accumulation in rat hepatoma cells.** ***J. Lipid Res.*** **2010.** 51: **368–377.**

Supplementary key words lipase • very low density lipoprotein • endoplasmic reticulum • β-oxidation

Hydrolysis of hepatic intracellular triacylglycerol (TG) stores generates substrates for β-oxidation and lipid resynthesis, some of which are utilized for the assembly of VLDLs (1–3). The assembly of VLDL involves both cotranslational and posttranslational addition of lipids to apolipoprotein B (apoB) (4–7). The transfer of lipids to nascent apoB particles is facilitated by the microsomal triglyceride transfer protein (8, 9). Microsomal triglyceride transfer protein is also responsible for the formation of apoB-free endoplasmic reticulum (ER) lumenal lipid droplets (10–12). These lipid droplets are believed to serve as lipid donors for bulk lipidation of primordial apoB-containing particles (10–13). One enzyme that has been implicated to play a role in the hydrolysis of stored TG pools and assembly of VLDL is an ER-associated triacylglycerol hydrolase (TGH) (14–20). Inhibition of TGH leads to decreased TG mobilization and apoB secretion from hepatocytes (15). However, treatment of hepatocytes with a TGH-specific inhibitor reduced secretion of TG and apoB to a lesser extent than the general lipase inhibitor, diethyl *p*-nitrophenyl phosphate (E600), suggesting that other lipases may also contribute to VLDL assembly (15). The fact that perinatal rat hepatocytes are capable of TG secretion in the absence of TGH expression in this particular developmental stage provides further support for the existence of additional lipases (21, 22).

In addition to VLDL assembly, fatty acids released from intracellular stores can be utilized for energy production via β-oxidation in the mitochondria. Unlike the well-described roles of adipose triglyceride lipase (ATGL) and hormone-sensitive lipase (HSL) in the mobilization of TG stores in adipose tissue (23–26), the identity of hepatic lipases supporting β-oxidation is still unclear. Arylacetamide deacetylase (AADA) shares sequence homology with HSL (27) and possesses a classical lipase/esterase GXSXG active site motif (27, 28). Trickett et al. (28) have shown that hepatic AADA mRNA levels follow a diurnal rhythm with an identical pattern to hepatic VLDL secretion in mice. In this study, we

This work was supported by a Grant-in-Aid from the Heart and Stroke Foundation of Alberta, Northwest Territories, and Nunavut. V.L., B.E., and M.T.-H. were supported by the Canadian Institutes of Health Research/Heart and Stroke Foundation of Canada/Industry Stroke, Cardiovascular, Obesity, Lipid, Atherosclerosis Research Strategic Training Program. R.L. is a senior scholar of the Alberta Heritage Foundation for Medical Research.

Manuscript received 31 July 2009 and in revised form 3 August 2009.

Published, JLR Papers in Press, August 3, 2009
DOI 10.1194/jlr.M000596

Abbreviations: AADA, arylacetamide deacetylase; apoB, apolipoprotein B; ASM, acid-soluble metabolite; ATGL, adipose triglyceride lipase; CE, cholesteryl ester; CNX, calnexin; DG, diacylglycerol; E600, diethyl *p*-nitrophenyl phosphate; ECL, enhanced chemiluminescence; Endo H, endoglycosidase H; ER, endoplasmic reticulum; HSL, hormone-sensitive lipase; McA, McArdle-RH7777; 4-MUH, 4-methyl umbelliferyl heptanoate; OA, oleic acid; PC, phosphatidylcholine; PL, phospholipids; PNGase F, glycopeptidase F; pNP, *p*-nitrophenyl; TG, triacylglycerol; TGH, triacylglycerol hydrolase; T-TBS, Tris-buffered saline containing 0.2% Tween 20.

[1]To whom correspondence should be addressed.
e-mail: richard.lehner@ualberta.ca

examined whether AADA influences lipid metabolism in McArdle-RH7777 (McA).

MATERIALS AND METHODS

Materials

E600, 4-methyl umbelliferyl heptanoate (4-MUH), *p*-nitrophenyl acetate (pNP-acetate), oleic acid (OA), and essentially fatty-acid-free BSA were obtained from Sigma (St. Louis, MO). 6-*N*-biotinylaminohexyl isopropyl phosphofluoridate (FP-biotin) was from Toronto Research Chemicals (Toronto, ON, Canada). [9,10(*n*)-^{3}H]oleic acid (7 Ci/mmol) was from Amersham (Oakville, ON, Canada). Primary antibodies were from the following sources: mouse anti-FLAG M2 (Stratagene, La Jolla, CA), anti-Calnexin (Stressgen Biotechnologies, Victoria, BC, Canada), and goat anti-apoB (Chemicon, Temecula, CA). Secondary antibodies were from the following sources: avidin-HRP from Bio-Rad (Mississauga, ON, Canada) and goat anti-rabbit HRP from Pierce Biotechnologies (Brockville, ON, Canada).

Cloning the chimeric AADA cDNA

Two oligonucleotides were synthesized corresponding to the cDNA sequence of mouse AADA. The forward primer contained sequence of the coding region of the cDNA (5′-ATGGGGAAAACCATTTCTCTTCTC-3′). The reverse primer corresponded to the complementary strand (5′-TTACAGATTTTTGATAAGCCAACTCAA-3′). These primers were used to amplify the AADA cDNA (~1.2 kb) from a mouse liver λgt11 cDNA library using *Pwo* polymerase (Roche). Amplification was performed at 93°C for 1 min, 60°C for 1 min, and 72°C for 2 min for 30 cycles. The PCR product was ligated into the *Eco*RV site of pBluescript II SK− plasmid, and the entire cDNA was sequenced. This plasmid was used as a template to generate a chimeric cDNA encoding the mouse AADA protein with a FLAG epitope at the extreme C terminus (AADA-FLAG). The forward primer for AADA-FLAG (5′-GCAGCTCGAGATGGGGAAAACCATTTCTCTTCTCATCTC-3′) contained sequence of the coding region of AADA and the *Xho*I restriction site (underlined). The reverse primer for AADA-FLAG (5′-TCATTCTAGATCA-**CTTATCGTCGTCATCCTTGTAATC**CAGATTTTTGATAAGCCAACTCAAGTACTG-3′) corresponding to the complementary strand, introduced the FLAG sequence (bold) immediately before the stop codon and the *Xba*I restriction site (underlined) following it. AADA-FLAG was amplified with *Taq* polymerase (Invitrogen), cloned into the pCR4-TOPO plasmid (Invitrogen), and sequenced. The chimeric cDNA was excised from this plasmid using *Xho*I and *Spe*I and was ligated into *Xho*I- and *Xba*I-digested pCI-neo (Promega) mammalian expression vector.

Cell culture and generation of McA cell lines stably expressing AADA-FLAG cDNA

McA cells, obtained from ATCC, were cultured in DMEM containing 50 units/ml penicillin/streptomycin, 10% horse serum, and 10% FBS at 37°C in humidified air containing 5% CO_2. Wild-type McA cells were transfected with 6 μg of empty vector pCI-neo (pNeo) or AADA-FLAG-pCI-neo using Lipofectamine2000. Transfected cells were grown in media with 1.6 mg/ml G-418 for 5 days to select for neomycin resistance. Individual clones were isolated and analyzed for AADA-FLAG protein by Western blotting. Stable cell lines, designated pNeo, A13, and A23, were thereafter maintained in media containing 0.4 mg/ml G-418.

Preparation of cellular membranes

Cells from 100 mm culture dishes grown to ~70% confluency were harvested into 2 ml of PBS (137 mM NaCl, 2.7 mM KCl, 10 mM Na_2HPO_4, and 2 mM KH_2PO_4). Cells were disrupted by sonication and spun at 2,500 *g* for 5 min to isolate cell debris. The supernatant was subjected to ultracentrifugation for 45 min at 360,000 *g* to isolate cell membrane fractions.

Activity-based probe labeling

FP-biotin covalently modifies active site serine residue in serine hydrolases (29). FP-biotin was dissolved in DMSO to obtain a 10 mM stock. McA cell membranes (30 μg protein) in 20 mM Tris, pH 7.0, 150 mM NaCl, and 1 mM EDTA were adjusted to 1.5 mM (0.07%) Triton X-100 and reacted with 100 μM FP-biotin for 30 min at room temperature. The sample was then boiled in SDS-PAGE loading buffer and separated by SDS-PAGE. Following transfer to nitrocellulose, biotinylated proteins were visualized by probing with avidin-HRP and enhanced chemiluminescence (ECL).

Lipase and esterase assays

Carboxylester hydrolase activities in membrane fractions isolated from pNeo and AADA-FLAG stable cell lines were determined by measuring the hydrolysis of 4-MUH and pNP-acetate (30). Membrane fractions from McA cells expressing human TGH were used as a positive control for both esterase and lipase assays (16, 31). Protein concentrations were determined with Protein Assay Reagent (Bio-Rad Laboratories) according to the manufacturer's instructions.

Lipolysis of membrane-associated lipids, McA cells (stably transfected with either pNeo or AADA), were incubated for 4 h with serum-free DMEM containing 0.4 mM OA complexed to 0.4% BSA and [9,10(*n*)-^{3}H]OA as radiolabeled tracer to stimulate lipid synthesis. Cells were washed with ice-cold PBS and harvested in ice-cold homogenization buffer (250 mM sucrose and 50 mM Tris, pH 8.0), disrupted by Potter Elvehjem homogenizer, and microsomal membranes were prepared from postnuclear supernatants by 1 h centrifugation at 106,000 *g*. Microsomes containing radiolabeled lipids were suspended in homogenization buffer and incubated for up to 4 h at 37°C. Lipids were extracted and radioactivity phosphatidylcholine (PC), diacylglycerol (DG), FAs, and TGs were determined following TLC as described below.

Measurements of OA incorporation into cellular lipids

McA pNeo, A13, and A23 cell lines were grown to ~70% confluency in 60 mm culture dishes. Cells were incubated for 4 h with 2 ml of serum-free DMEM containing 0.4 mM OA complexed to 0.4% BSA (14) in the presence or absence of 100 μM E600. After 4 h OA loading, cells were washed with ice-cold PBS, harvested in 2 ml of the same buffer, and disrupted by sonication. Lipids from cell lysates were extracted, and TG, cholesteryl esters (CEs), and phospholipids (PLs) were quantified by gas chromatography (32).

Metabolic labeling studies

McA pNeo, A13, and A23 cell lines were grown to ~70% confluency in 60 mm culture dishes. Cells were pulse labeled for 4 h with 2 ml of serum-free DMEM containing 0.4 mM OA complexed to 0.4% BSA and [9,10(*n*)-^{3}H]OA as radiolabeled tracer to stimulate neutral lipid synthesis. Some dishes from each cell line contained 100 μM E600 to inhibit lipase activity. After 4 h pulse, some cells and media were collected for analyses. For the remaining dishes of cells, the pulse media were aspirated, cells were washed three times with serum-free DMEM containing 0.4% fatty acid free BSA and then incubated with 2 ml of serum-free DMEM for additional 4 h, which represented the 4 h chase period. Some dishes from each cell line were also incubated in the presence of 100 μM E600 to inhibit lipase activity. After 4 h chase,

cells and media were collected for analyses as described above. The media were centrifuged at 2,500 *g* for 5 min to remove cell debris. All cells were washed with ice-cold PBS, harvested in the same buffer, and disrupted by sonication. Cellular and media lipids were extracted by the method of Folch, Lees, and Sloane Stanley (33) in the presence of lipid carriers. The lipids were spotted on TLC plates and resolved with a two-solvent system as described previously (14, 15) before visualization by exposure to iodine. Incorporation of radioactivity into TG, CE, and PC were recovered and their radioactive contents were determined by scintillation counting.

Fatty acid oxidation measurements

Media obtained from the metabolic labeling studies were analyzed for content of acid-soluble metabolites (ASMs) released from the cells during β-oxidation. Thirty microliters of 20% BSA and 16 μl of 70% perchloric acid were added to 200 μl of culture media from each cell line. Media were then centrifuged at 25,000 *g* for 5 min before an aliquot of the supernatant was counted for radioactivity. These experimental conditions were adapted from studies conducted by Hansson et al. (34).

Secretion of apoB

Media were collected at the end of 4 h OA loading and then centrifuged at 2,500 *g* for 10 min to isolate cell debris. ApoB was immunoprecipitated from media equivalent to 0.5 mg of cell protein. Following overnight incubation in 0.1% SDS, 0.5% deoxycholate, 1% Triton-X-100, protease inhibitors, 4 μL of goat anti-apoB antibodies, and 10 μL of protein A Sepharose were added to each sample, and the suspensions were incubated for 4 h at 4°C. Sepharose beads were pelleted by brief centrifugation and washed three times with PBS. Samples were resuspended in SDS-PAGE loading buffer before proteins were resolved by SDS-PAGE and transferred to nitrocellulose membranes. Membranes were blocked with 5% skim milk in TBS containing 0.2% Tween 20 (T-TBS) and then incubated with 1:5,000 dilution of goat anti-apoB primary antibodies followed by incubations with 1:10,000 dilution of HRP-conjugated rabbit anti-goat secondary antibodies. Immunoreactivity was detected by exposures to Biomax MR film (Kodak) after using ECL Western Blotting Detection Reagents.

Generation of AADA polyclonal antibodies

Antibodies against mouse AADA were obtained by immunization of rabbits with the C-terminal 14 amino acids of mouse AADA linked to keyhole limpet hemocyanin. Briefly, rabbits were injected subcutaneously with an initial dose of 0.5 mg of the conjugated peptide in complete Freund's adjuvant followed by three booster injections of 0.2 mg of the conjugated peptide at 3-week intervals. Preimmune and anti-AADA sera were prepared, aliquoted, and stored at −80°C.

Immunoblotting of AADA

Proteins were resolved by SDS-PAGE, transferred to nitrocellulose membranes, and immunoblotted. All membranes were blocked with 5% skim milk in T-TBS for 1 h prior to antibody incubations. All antibody incubations were carried out in 1% skim milk solution in T-TBS. Cellular membrane proteins prepared from McA cell lines or mouse liver homogenates were separated by 10% polyacrylamide SDS gels and transferred to nitrocellulose membranes. The membranes were blocked with TBS-0.1% Tween 20-5% milk and then were incubated with: 1:10,000 dilution of mouse anti-FLAG primary antibodies followed by 1:10,000 dilution of HRP-conjugated goat anti-mouse secondary antibodies or 1:1,000 dilution of rabbit anti-AADA primary antibodies or 1:10,000 dilution of rabbit anti-Calnexin primary antibodies followed by 1:10,000 dilution of HRP-conjugated goat anti-rabbit secondary antibodies. All immunoblots were exposed to BioMax MR film after using ECL Western Blotting Detection Reagents.

Glycopeptidase F and endoglycosidase H treatments

For glycopeptidase F (PNGase F) treatment, cell lysates were prepared from the A13 McA cell line by homogenization in 100 mM Tris-HCl, pH 8.0. Ten microliters of 10% SDS, 10 μl of 10% Triton X-100, and 2 μl of 2-mercaptoethanol were added to 100 μL of cell lysates, and samples were boiled for 5 min and cooled on ice for 20 min. Half of each sample was treated with 2 μL (10 units) of PNGase F and the other half with 2 μl of Tris buffer (control). Samples were incubated overnight at 37°C for deglycosylation and then boiled in 1× SDS-PAGE loading buffer and resolved by 10% SDS-PAGE. AADA was visualized by immunoblotting with anti-AADA sera.

For endoglycosidase H (Endo H) treatments, cell lysates were prepared from the A13 McA cell line by homogenization in TBS containing 2% Triton X-100. One hundred microliters of 100 mM sodium citrate, pH 5.5, were added to 100 μL of cell lysates followed by 10 μL (50 mU) of Endo H to half of each sample, and 10 μL of sodium citrate buffer (control) were added to the other half. Samples were incubated overnight at 37°C for deglycosylation. Samples were boiled for 5 min in 1× SDS-PAGE loading buffer and resolved by 10% SDS-PAGE. AADA was visualized by immunoblotting with anti-AADA sera.

Animal care

All procedures were approved by the Animal Care and Use Committee at the University of Alberta and were in accordance with guidelines of the Canadian Council on Animal Care. Male adult mice from C57BL/6J background were used for experiments. Mice were fed ad libitum a chow diet (Lab Diet; PICO Laboratory Rodent Diet 20) and were exposed to a 12 h light/dark cycle starting at 8 AM. Hepatocytes were prepared in the morning from fed mice by collagenase perfusion of the livers.

Confocal immunofluorescence imaging

Mouse hepatocytes isolated from wild-type C57BL/6J mice were grown on collagen coated coverslips in 6-well dishes with DMEM containing 10% HS and 10% FBS overnight. Cells were fixed with 4% paraformaldehyde in PBS for 10 min at room temperature, permeabilized with 0.2% Triton X-100 in PBS for 5 min at room temperature, and then subjected to antibody incubations. Cells were incubated with rabbit anti-AADA sera and mouse anti-PDI antibodies at 1:100 dilution in 3% BSA in PBS for 1 h. Samples were then incubated with Alexa 488-conjugated goat anti-rabbit and Texas Red-conjugated donkey anti-mouse secondary antibodies at 1:100 dilution in 3% BSA in PBS for 1 h. After rinsing coverslips three times with PBS, the coverslips were mounted on glass slides with Prolong® Antifade Kit mounting medium and stored at 4°C. All slides were viewed by a Zeiss LSM510 confocal microscope (Carl Zeiss Canada, Toronto, ON) and analyzed by the Zeiss LSM510 Image Browser software. Imaging of AADA-FLAG in transfected McA cells was performed similarly using anti-FLAG antibodies.

Subcellular fractionation

Livers harvested from wild-type C57BL/6J mice were homogenized in ice-cold homogenization buffer (10 mM Tris-HCl at pH 7.4, 250 mM sucrose, 5 mM EDTA, and 1× complete protease inhibitor cocktail; Roche Diagnostics, Indianapolis, IN). The ho-

mogenate was subjected to centrifugation at 10,000 *g* for 10 min to obtain postnuclear supernatant. A Nycodenz gradient (Histodenz; Sigma-Aldrich, Oakville, ON, Canada) was performed by loading in order from top to bottom, 2.5 ml of 10, 14.66, 19.33, and 24% Nycodenz stock solution in 10 mM Tris-HCl, pH 7.4, 3 mM KCl, 1 mM EDTA, and 0.02% NaN_3 (35). The tube containing this Nycodenz gradient was then sealed with parafilm and placed horizontally at room temperature for 45 min and then centrifuged at 169,000 *g* for 4 h at 15°C in a SW41 rotor in order to create a nonlinear gradient. Once the gradient was formed, the postnuclear supernatant was applied on top of the gradient and then subjected to centrifugation at 169,000 *g* for 1.5 h at 15°C. After centrifugation, 15 800-µL fractions were isolated from the gradient, and 160 µL from each fraction was subjected to acetone precipitation by the addition of 640 µL of acetone (a volume equivalent to 4 times the volume of the samples) and incubated for 1 h at −20°C. The samples were spun at 13,000 *g* for 10 min to pellet the precipitated proteins. The supernatant was removed and the pellets were resuspended in 50 µL of 1× SDS-PAGE loading buffer, boiled for 5 min, and then separated by SDS-PAGE. Proteins were transferred to nitrocellulose membrane and immunoblotted for AADA, an ER marker calnexin (CNX), and a Golgi marker TGN.

Statistical analysis

Comparisons between three groups (control and two AADA-expressing cell lines) were analyzed by one-way ANOVA using the software GraphPad PRISM® 4. All values are presented as means ± SD. Statistically significant differences between means were denoted as those with values of $*P < 0.001$, $**P < 0.01$, and $***P < 0.05$.

RESULTS

Localization of AADA in mouse liver and expression of FLAG-tagged AADA in McA cells

AADA colocalizes with a known ER marker protein disulfide isomerase in primary mouse hepatocytes as determined by indirect immunofluorescence staining and confocal microscopy (**Fig. 1A**). The ER localization was confirmed by Nycodenz density fractionation of mouse liver homogenate, where AADA cofractionated with another ER resident protein CNX and was absent from Golgi fractions containing TGN-38 (Fig. 1B). Mouse AADA cDNA encoding the FLAG epitope engineered just prior to the stop codon was cloned into a pCI-neo plasmid and stably transfected into McA cells, which do not express endogenous AADA (Fig. 1C, E). Immunoblots of total cell membrane fractions prepared from FLAG-tagged AADA-expressing McA cells with anti-FLAG antibodies (Fig. 1D) and with antibodies raised against the C-terminal 14 amino acid peptide of mouse AADA (Fig. 1E) revealed an immunoreactive band of expected molecular mass (50 kDa) that was not present in membranes isolated from the empty vector transfected McA (Fig. 1D, E). The levels of AADA protein in the two cell lines used for further experiments (cell lines A13 and A23) were significantly lower than that present in mouse liver fractions (Fig. 1E). Higher expression of AADA in McA cells could not be obtained for unknown reasons. The lower levels of AADA in McA cells compared with liver were not due to increased degradation of the AADA protein, but due to lower level of mRNA expression as measured by quantitative real-

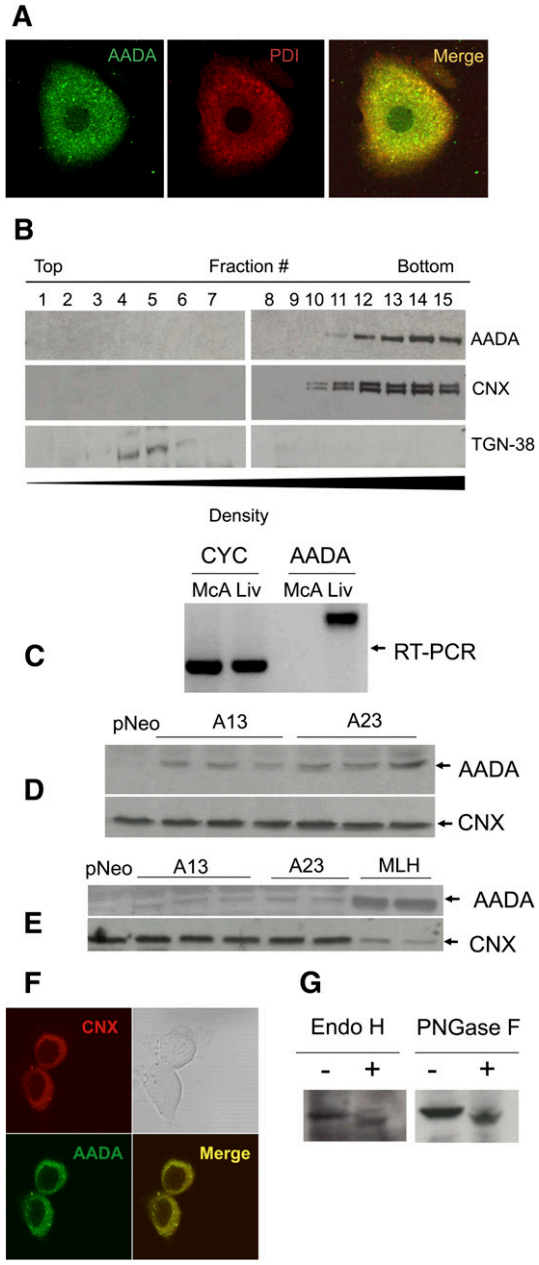

Fig. 1. Localization and expression of mouse AADA. A: Localization of endogenous AADA in primary mouse hepatocytes by confocal immunofluorescence microscopy. B: Subcellular fractionation of mouse liver homogenate. AADA was detected with anti-mouse AADA polyclonal antibodies as described in Materials and Methods. C: AADA is expressed in rat liver but not in rat-derived McA cells as determined by RT-PCR. CYC, cyclophilin (control); Liv, liver. D: Twenty micrograms of membrane proteins prepared from individual dishes of McA cells stably transfected with an empty pCI-neo vector or pCI-neo vector containing FLAG-tagged mouse AADA cDNA (A13 and A23) were electrophoresed in SDS-PAGE, proteins were transferred to a nitrocellulose membrane and immunoblotted with anti-FLAG and anti-CNX (loading control) antibodies as described in Materials and Methods. E: Twenty micrograms of membrane protein from stably transfected McA cells and from mouse liver homogenate (MLH) were electrophoresed, transferred to a nitrocellulose membrane, and immunoblotted with anti-mouse AADA and anti-CNX antibodies as described in Materials and Methods. F: Localization of AADA in transfected McA cells by confocal immunofluorescence microscopy. G: Cell lysates from AADA-expressing cells were treated with deglycosylation enzymes and changes in AADA molecular mass was assessed by SDS-PAGE.

time PCR (data not shown). AADA in transfected McA cells was properly targeted to the ER as determined by colocalization with CNX (Fig. 1F). Mouse AADA contains one possible N-glycosylation site (N_{280}WSS). Treatments of cell lysates prepared from AADA-expressing cells with either PNGase F or Endo H increased AADA mobility in SDS-polyacrylamide gels (Fig. 1G), indicating that the expressed AADA is a glycoprotein with a Type II membrane topology.

Determination of esterase/lipase activity of AADA

To address whether AADA cDNA encodes functional carboxyl ester hydrolase, we utilized pNP-acetate (water-soluble esterase substrate) and 4-MUH (water-insoluble esterase substrate) to monitor hydrolytic activities in microsomes prepared from McA cells transfected with AADA cDNA. A13 and A23 microsomal fractions exhibited increased esterase activities against both of these substrates (**Fig. 2A**, B). The in vitro activity of AADA against these substrates appeared comparable to that seen in microsomes prepared from McA cells expressing similar levels of TGH protein (based on binding of activity-based probe; see below). Detergent-free liposomal preparations of lipids used for assaying cytosolic lipases, such as HSL or ATGL, are not suitable substrates for AADA because these liposomal preparations cannot cross the ER membrane bilayer to gain access to the lumenally oriented AADA. AADA-containing microsomes also did not show any increase in hydrolysis of detergent solubilized lipids (TG, CE, PLs, or oleoyl-CoA) compared with microsomes isolated from control (empty vector transfected) cells. We therefore decided to assess lipolytic AADA activity against endogenously synthesized [^{3}H]oleate-labeled lipids. During 4 h incubation of [^{3}H]OA-labeled microsomes, the presence of AADA did not increase hydrolysis of endogenously synthesized glycerophospholipids or TG (data not shown); however, diacylglycerol appeared to undergo increased turnover. At the end of the 4 h incubation, AADA microsomes contained 28% less radiolabeled DG compared with time 0, while DG label in pNeo microsomes was not altered during this incubation period (Fig. 2C). Microsomes isolated from AADA cells that were incubated with [^{3}H]OA also contained approximately 30% less radiolabeled DG compared with mock transfected cells. The presence of the nucleophilic active serine residue in AADA was determined by incubations with the serine hydrolase activity-based probe FP-biotin that specifically covalently binds to active serine in esterases and lipases. A 50 kDa protein corresponding to AADA was labeled in AADA-expressing cell homogenates but not in control cell homogenates (Fig. 2D). This result strongly suggests that the expressed AADA is a catalytically active esterase and that the observed increases in in vitro activities against artificial and native substrates are due to the enzymatic activity of AADA rather than to its potential auxiliary role in hydrolysis. McA cells stably transfected with human TGH cDNA were utilized as a positive control for the FP-biotin reactivity since TGH is a known active serine esterase and has been previously identified in FP-labeling studies (29).

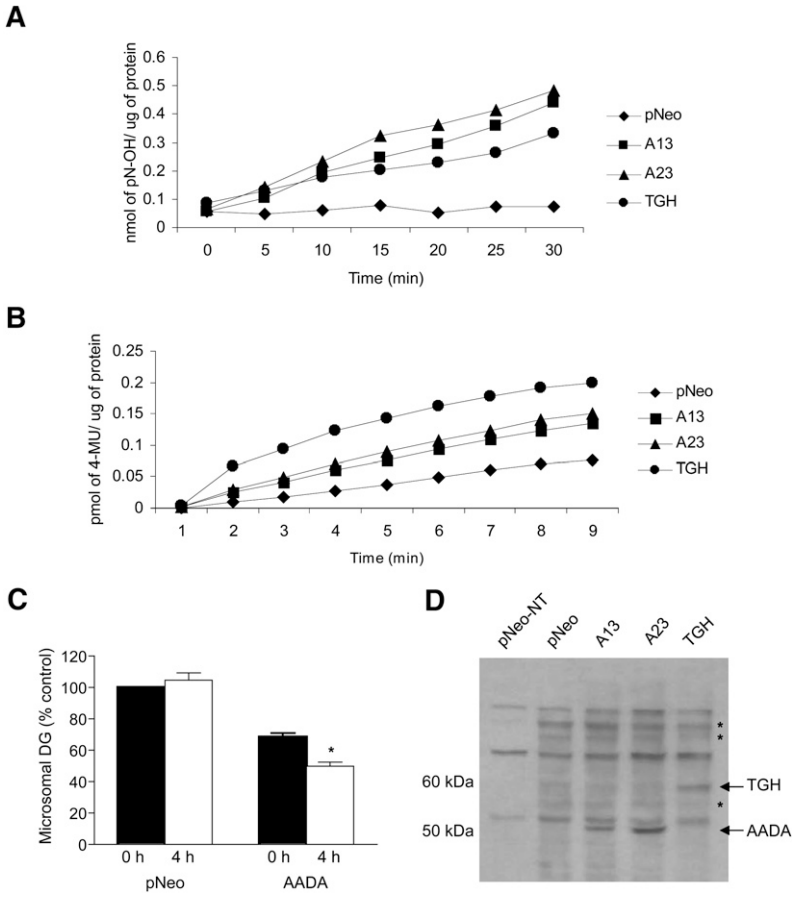

Fig. 2. AADA hydrolyzes soluble and insoluble carboxylesters. Twenty micrograms of membrane protein prepared from McA cells stably transfected with an empty pCIneo vector, FLAG-tagged mouse AADA, or human TGH cDNAs were incubated with pNP-acetate (A) or 4-MUH (B). The release of pNP was monitored at 405 nm and that of 4-umbelliferyl at 460 nm. The results are presented as an average from triplicate measurements. C: Hydrolysis of microsomal lipids. Cells were incubated with radiolabeled oleic acid, and microsomes were isolated and incubated for 4 h as described in Materials and Methods. Lipids were extracted and resolved on TLC plates, and radioactivity was determined by scintillation counting. Data (mean ± SD) from three separate experiments performed in triplicate are presented with radioactivity in DG in pNeo microsomes at time 0 set as 100%. Equal amounts of microsomal protein were used for the assay. The actual starting dpm in microsomal lipid fractions at time 0 were 22,000–25,000 for PC, 12,000–18,000 for TG, and 1,500–2,300 for DG. D: Thirty micrograms of total cellular membrane proteins from McA cells stably transfected with pCI-neo, A13, A23, and human TGH were either not treated (pNeo-NT) or treated with FP-biotin, resolved in SDS-PAGE, and transferred to nitrocellulose membrane, and biotinylated proteins were visualized with streptavidin-HRP. Asterisks indicate other potential endogenous serine hydrolases present in McA cells.

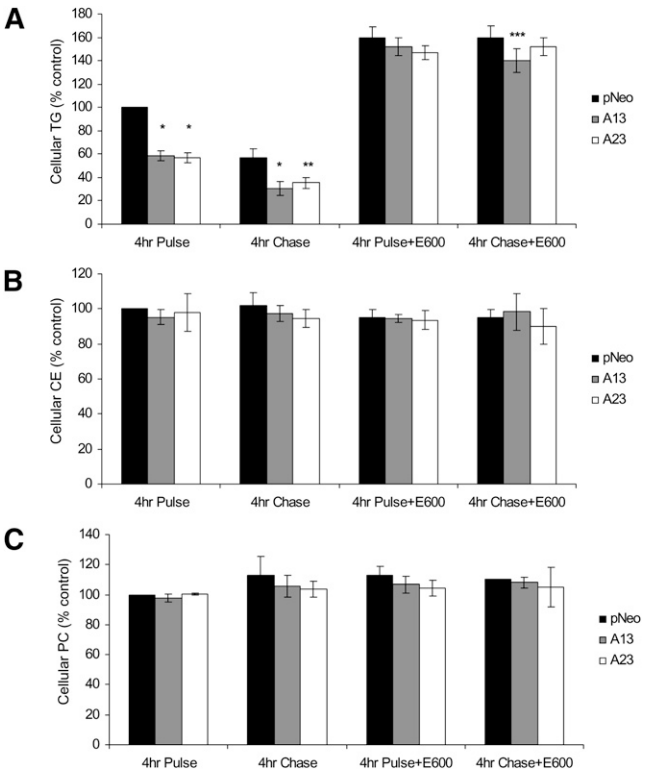

Fig. 3. AADA expression decreases levels of de novo synthesized TG. McA cells stably transfected with an empty pCI-neo plasmid or pCI-neo plasmid containing FLAG-tagged mouse AADA cDNA (A13 and A23) were incubated with 0.4 mM [^{3}H]OA in the presence or absence of a lipase inhibitor E600 and harvested either after pulse or chase as indicated. Lipids were extracted and analyzed by TLC as described in Materials and Methods. The amount of radioactivity incorporated into TG (A), CE (B), and PC (C) was determined by scintillation counting. Due to slight variation in radioactivity incorporation in three independent experiments, the data presented are shown as percentages of the dpm counts per milligram of protein of control pCI-neo at 4 h pulse. The actual dpm/mg cell protein incorporated into cellular lipids for pCI-neo at 4 h pulse from three independent experiments performed in triplicates (mean ± SD) were between 150,000 ± 30,000 and 190,000 ± 20,000 for TG, 50,000 ± 9000 and 71,000 ± 6300 for CE, and 100,000 ± 5500 and 110,000 ± 26,000 for PC. *P < 0.001, **P < 0.01, and ***P < 0.05 compared with pCI-neo (pNeo) cells.

AADA-expressing McA cells accumulates less intracellular TG

Four hour pulse incubations of pNeo cells with 0.4 mM [^{3}H]OA led to cellular accumulation of radiolabeled TG (**Fig. 3A**). However, AADA-expressing cells contained significantly less TG than the control pCI-neo cells (~40% decrease, $P < 0.001$). Differences in intracellular TG were abolished when the incubation mixture was supplemented with the lipase inhibitor E600 (Fig. 3A), indicating that the decrease in TG levels in AADA-expressing cells was due to lipolytic activity of the enzyme rather than any possible effect(s) on fatty acid uptake and/or TG synthetic enzymes. Fatty acid uptake into the pNeo and AADA cells was not found to be different during 15, 30, 45, and 60 min incubation of the cells with 0.4 mM [^{3}H]OA (data not shown). The specificity of the effect of AADA on lipolysis rather than synthesis was further evidenced by similar levels of PC and CE synthesis among the cell lines (Fig. 3B, C). Besides removing any difference in TG levels among cell lines, addition of E600 in the 4 h pulse incubation resulted in increased of TG accumulation in all cell lines (60% by control cells and 150% by AADA-expressing cells), suggesting that all active TG mobilization in the McA cells has been blocked effectively and TG synthesis is equivalent in control and AADA-expressing cells. During the subsequent 4 h chase incubations of cells in the absence of exogenous OA, the preformed TG was turned over rapidly in the absence of the lipase inhibitor. About 42% of the radiolabeled TG was depleted in the 4 h chase, and this turnover rate was similar in the control and AADA-expressing cells (Fig. 3A), indicating that AADA did not likely participate in the turnover of preformed TG stores, but acted on newly synthesized lipids. Continued inclusion of E600 in the 4 h chase period has also inhibited turnover of preformed TG.

The reduction in TG labeling was also reflected by the decrease in total TG mass in AADA-expressing cells after treatment with 0.4 mM OA for 4 h when compared with control cells. In agreement with the results from metabolic labeling studies, both AADA cell lines were found to store significantly less intracellular TG (**Fig. 4A**). Similarly, addition of E600 was able to abolish the difference in intracellular TG levels between AADA and control cell lines. While a difference in intracellular TG accumulation between AADA-expressing and control cells was observed, intracellular CE levels increased about 200% in all cell lines in the presence of exogenous OA and did not differ among cell lines (Fig. 4B), whereas PL levels remained relatively constant (Fig. 4C). These results further support the role of AADA in the regulation of cellular TG levels.

ApoB and TG secretion is decreased as a result of AADA expression in McA cells

The observed decrease in intracellular TG levels in AADA-expressing cells could have been due to increased secretion of this lipid as part of apoB-containing lipoproteins. Therefore, we wished to determine whether AADA expressing cells secreted more TG in apoB-containing particles. Densitometry analysis of immunoblots of media apoB revealed that expression of AADA led to decreased apoB100 secretion (**Fig. 5A, B**). In addition, analyses of media lipids from metabolic labeling studies showed that TG secretion was also lower in AADA-expressing cells (Fig. 5C). About 3.8% of newly synthesized TG was secreted during the 4 h OA incubations from control compared with 2.4% (37% decrease vs. control) and 2.7% (30% decrease vs. control) from A13 and A23 AADA-expressing cells, respectively. This suggests that AADA cells not only secreted a decreased amount of TG, but also exhibited a lower rate of secretion of de novo synthesized TG. On the other hand, during the 4 h chase period, which represents the secretion of preformed TG, all cell lines secreted about 0.7% of cellular TG that had accumulated at the end of the pulse period (data not shown). This reveals that AADA did not influence the rate of secretion of stored TG from McA cells. These results suggest that the increased hydro-

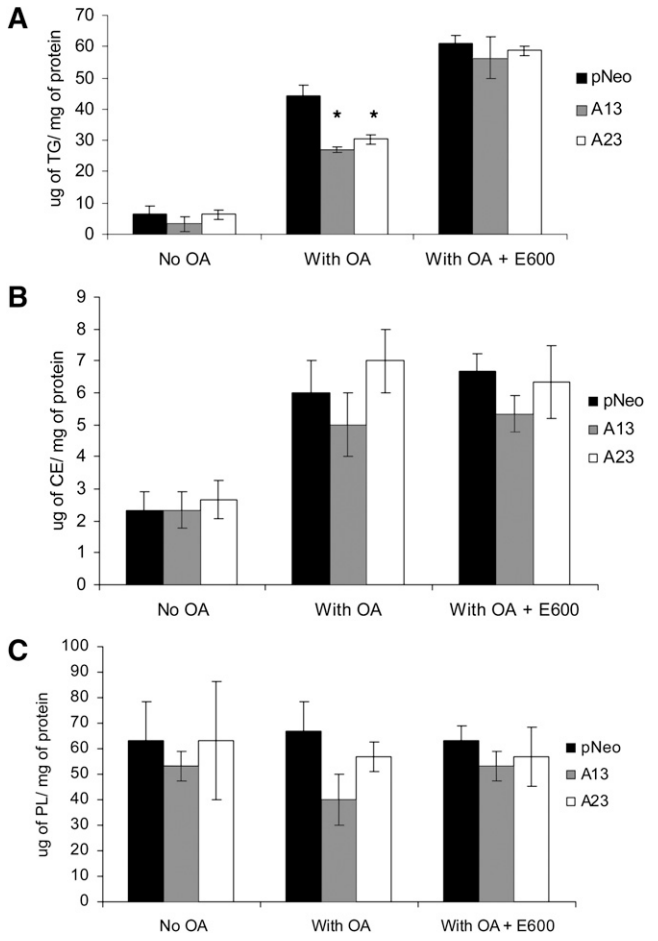

Fig. 4. AADA expression decreases cellular TG mass levels. McA cells stably transfected with an empty pCI-neo vector or pCI-neo vector containing FLAG-tagged mouse AADA cDNA (A13 and A23) were incubated in serum-free DMEM in the presence or absence of 0.4 mM OA and in the presence or absence of a lipase inhibitor E600 for 4 h. Cells were harvested in 2 ml of ice-cold PBS, lipids were extracted, and the mass of TG (A), CE (B), and phospholipids (PL) (C) was measured by gas chromatography as described in Materials and Methods. The data presented are representative of two independent experiments performed in triplicates. $*P < 0.001$.

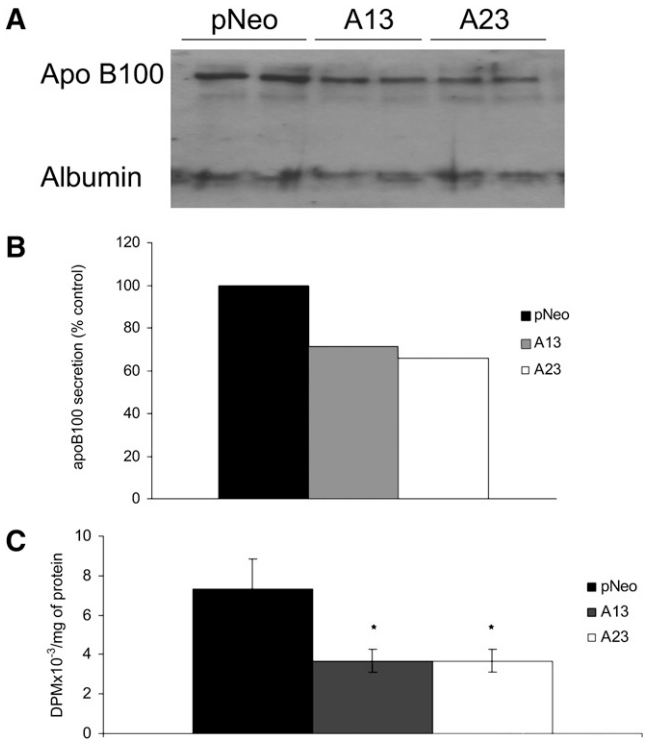

Fig. 5. AADA expression decreases apoB and TG secretion. A: Media from 100 mm dishes of McA cells stably transfected with an empty pCI-neo vector or pCI-neo vector containing FLAG-tagged mouse AADA cDNA (A13 and A23) were collected after 4 h incubation with 0.4 mM OA. The samples were incubated with anti-apoB antibodies, and then the antigen-antibody complexes were bound to protein A Sepharose. Collected immunoprecipitates were electrophoresed in SDS-PAGE and immunoblotted with anti-apoB antibodies as described in Materials and Methods. B: Densitometry analysis of the amount of apoB100 secretion is expressed as a percentage of apoB secreted by the control cell line (pCI-neo). C: McA cells were incubated with 0.4 mM [^{3}H]OA for 4 h. Cell media were subjected to lipid extraction and analysis. The amount of TG in media was measured by scintillation counting following TLC. The results in A and B are representative of four independent experiments. The results in C represent mean ± SD from three independent experiments performed in triplicates. $*P < 0.001$.

lysis of newly made lipids in AADA cell lines did not lead to increased channeling of substrates for VLDL assembly.

Increased fatty acid oxidation in AADA expressing cells

In order to determine whether the released fatty acids from newly made TG were utilized for fatty acid oxidation, the amount of ASMs released into the media at the end of 4 h pulse/chase experiments was quantified. ASM release reflects the level of fatty acid oxidation in cells. The level of ASM in media was augmented upon expression of AADA, which indicated an increase in fatty acid oxidation due to AADA expression (**Fig. 6**). During the 4 h chase period in the absence of exogenous fatty acids, the levels of fatty acids released from preformed stores for oxidation decreased by a similar percentage among the cell lines, suggesting that AADA has either no role or a very minor role in the mobilization of preformed TG stores for this process. Inclusion of E600 during the pulse incubations ablated the increase in β-oxidation in AADA cells, and the resultant ASM levels were similar in both control and AADA cells. Thus, it appears that in the presence of exogenous fatty acids, AADA activity provided additional 20% of the total fatty acids destined for β-oxidation, which was derived from hydrolysis of newly formed TG stores, and this mobilization could be blocked by lipase inhibitors. Since the delivery of exogenous fatty acids for β-oxidation in the presence of E600 is the same in control and AADA cells, this result provides additional evidence that fatty acid uptake by both control and AADA cells is similar, as seen in the cell labeling and lipid mass studies (Figs. 3C, 4B, respectively).

DISCUSSION

Increased flux of fatty acids to the liver from adipose tissue during fasting is a physiologically important process, and the liver readily metabolizes this energy source to

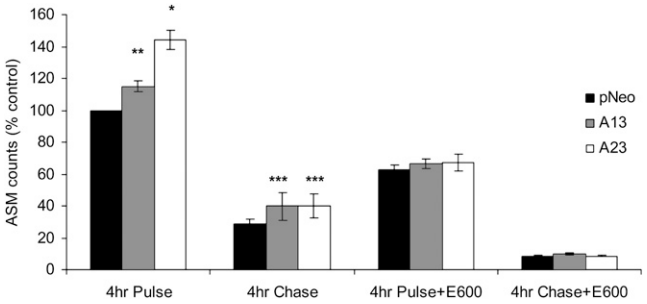

Fig. 6. AADA expression increases fatty acid oxidation. McA cells stably transfected with an empty pCI-neo vector and pCI-neo vector containing FLAG-tagged mouse AADA cDNA (A13 and A23) were incubated with 0.4 mM [^{3}H]OA for 4 h in the presence or absence of a lipase inhibitor E600 (pulse), followed by incubation in DMEM with or without a lipase inhibitor E600 (Chase). Media equivalent to 500 μg of cell protein were analyzed for radioactivity in ASMs as described in Materials and Methods. Due to slight variation in radioactivity incorporation in three independent experiments, the data presented are shown as percentages of control pCI-neo at 4 h pulse. The averages of the actual dpm/mg cell protein in ASM for pCI-neo at 4-h pulse from three independent experiments performed in triplicates (mean ± SD) were between 610,000 ± 70,000 and 880,000 ± 100,000. *$P < 0.001$, **$P < 0.01$, and ***$P < 0.05$.

maintain homeostasis. Fatty acids that enter the liver are reesterified into TG stores, which supply substrates for the assembly of VLDL or are utilized for β-oxidation. Both processes result in the provision of substrates that are used by other tissues during food deprivation. Ketone bodies that are formed from β-oxidation supply the brain with an energy source, and hepatic VLDL secretion provides fatty acids for energy production in the muscles. The majority of TG secreted with VLDL is derived from preformed hepatic TG stores through a process that involves lipolysis and reesterification (1–3). Although the mobilization of TG for VLDL secretion may represent an important regulatory step, there is paucity of information at the molecular level regarding the lipases responsible for this process. A well-studied adipose tissue lipase HSL is not appreciably expressed in the liver (36). Ectopic expression of this enzyme in hepatocytes resulted in increased mobilization of TG stores, and the released fatty acids were delivered to mitochondria for β-oxidation rather than for reesterification and VLDL assembly (37, 38). Another recently identified lipase, ATGL, has much broader tissue expression profile than HSL (23); however, its hepatic expression is also very low, and the role of this enzyme in hepatic lipid metabolism remains unknown (24). ATGL is activated by a lipid droplet-binding protein CGI-58 (39), and recent studies showed that overexpression of CGI-58 in McA cells increased VLDL secretion (40, 41). It is currently unclear whether the CGI-58-mediated effect is due to the regulation of ATGL that may be expressed in these cells or through another yet unidentified mechanism. From studies on HSL and ATGL overexpression in hepatic cells (37, 38), it is obvious that the localization of the lipases may determine the fate of the released fatty acids. Thus, hydrolysis of TG stores by cytosol-oriented lipases, such as HSL and ATGL, may channel fatty acids to mitochondria for oxidation (37, 38), while release of fatty acids in the ER could result in reesterification of the lipolytic products by ER-localized acyltransferases to support VLDL production. To date, two potential ER-localized lipases have been identified, AADA and TGH. While a positive role of TGH in hepatic VLDL assembly has been documented (14–17, 20), very little is known about the function of AADA. AADA was initially characterized through its drug transforming ability in vitro (27). Given its sequence homology to HSL, including conserved lipase/esterase catalytic triad residues, and its primary expression in organs responsible for lipid metabolism, AADA was hypothesized to have a role in hepatic lipid metabolism (28). Because HSL can hydrolyze a vast array of carboxylester substrates, including DG, TG, CE, as well as artificial esters (42), we postulated that AADA could also hydrolyze a variety of esters. This study has demonstrated that AADA exhibits hydrolytic activity against soluble and insoluble lipid esters and that cells expressing AADA cDNA have decreased cellular TG, but not cellular PC or CE levels. Addition of a lipase inhibitor E600 ablated the difference in intracellular TG levels between AADA and control cell lines, which also shows that the observed reduction in TG in AADA-expressing cells is due to AADA-mediated hydrolysis. The rate of turnover of preformed cellular TG (during the chase period) was similar between AADA-expressing and control cells, an indication that TG stored in cytoplasmic lipid droplets is not accessible to AADA.

Although AADA shares similarity with HSL and like HSL showed hydrolytic activity toward endogenously synthesized DG, we did not observe any in vitro activity of AADA toward membrane-associated TG or CE. Interestingly, AADA shares about 40% sequence identity (including 100% identity in the catalytic domain) with murine arylacetamide deacetylase-like 1 (also known as mKIAA1363 protein), which has been recently reported to possess CE hydrolase activity (43). Based on our findings, we propose a model where AADA hydrolyzes DG synthesized within the ER compartment (**Fig. 7**). However, we cannot eliminate the possibility at this time that AADA hydrolyzes other intermediates formed in the glycerol-3-phosphate pathway of glycerolipid synthesis. While DG is also a precursor for TG, PC, and phosphatidylethanolamine synthesis, we did not observe any changes in PC levels or PC synthesis in AADA-expressing cells. There is a precedent where ablation of enzyme activities within the glycerol-3-phosphate pathway lead to decreased TG but not glycerophospholipid synthesis. This has been observed through studies in mice deficient in the expression of glycerol-3-phosphate acyltransferase, acylglycerol-3-phosphate acyltransferase, and phosphatidic acid phosphohydrolase/lipin 1 (44–46). This can be explained by the presence of additional genes encoding duplicate catalytic activities for glycerolipid synthesis via the glycerol-3-phosphate pathway (46–49). It is also possible that AADA might hydrolyze acylglycerol intermediates, but enough DG is still produced to support the necessary glycerophospholipid synthesis, but not enough of this substrate is present to augment TG synthesis, which takes place when fatty acids and diacylglycerols

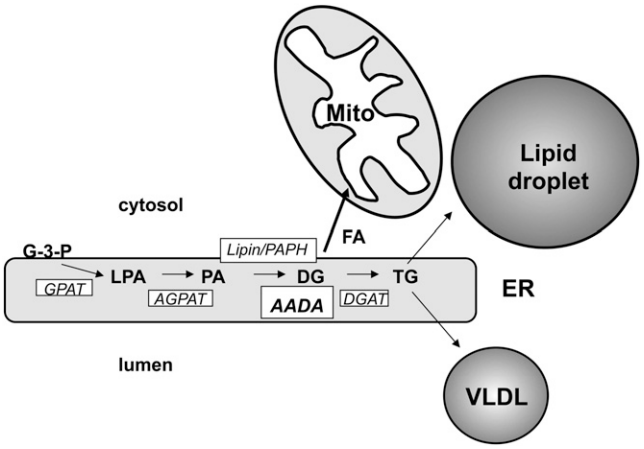

Fig. 7. Proposed role of AADA in the glycerol-3-phosphate pathway and its effect on hepatic lipid metabolism. TG is synthesized within the ER lipid bilayer by the enzyme of the glycerol-3-phosphate (also termed Kennedy) pathway. AADA hydrolyzes newly synthesized DG and provides fatty acids for β-oxidation in mitochondria (Mito). The result of AADA-mediated DG hydrolysis is the decreased amount of substrate for TG synthesis for cytoplasmic storage droplet formation and for VLDL assembly. AGPAT, 1-acylglycerol-3-phosphate acyltransferase; G-3-P, glycerol-3-phosphate; GPAT, glycerol-3-phosphate acyltransferase; LPA, lysophosphatidic acid; PA, phosphatidic acid; PAPH, phosphatidic acid phosphohydrolase.

are in excess. Another possibility would be that rather than hydrolyzing carboxylic esters, AADA could also function as a thioesterase and hydrolyze acyl-CoA, an obligate acyl-donor in glycerolipid biosynthesis. Existence of several pools of acyl-CoA within a cell has been postulated based on the presence of several isoforms of acyl-CoA synthetases catalyzing the fatty acid activation (50). Some of the acyl-CoA synthetases have been shown to participate in the synthesis of a specific lipid or lipid precursor (50), suggesting a possible formation of oligomeric complexes containing a specific acyltransferase and an acyl-CoA synthetase. It is plausible that such complexes could recruit a lipolytic enzyme as an additional regulatory switch; therefore, hydrolysis of specific acyl-CoA pools (for instance, one associated with TG synthesis) would not be expected to affect the synthesis of other lipids (for instance, glycerophospholipids and CE). However, membranes isolated from AADA-expressing cells did not exhibit increased acyl-CoA hydrolytic activity when compared with control membranes (data not shown), suggesting that acyl-CoA is not a substrate for the enzyme.

The decrease of cellular TG levels in AADA-expressing cells was accompanied by attenuated secretion of newly synthesized TG and increased fatty acid oxidation. Thus, AADA does not appear to participate in the lipolysis/reesterification cycle in support of VLDL assembly, but rather, AADA activity seems to limit the deposition of TG into cytosolic lipid droplet and VLDL. Interestingly, inhibition of lipase activity by E600 has lowered fatty acid oxidation in AADA-expressing cells to levels seen in control cells. This is the first time that a membrane-localized carboxylester hydrolase has been linked to the release of fatty acids for β-oxidation.

In conclusion, our results indicate that expression of AADA, even at levels substantially lower than those present in the liver, decreases intracellular TG levels, decreases VLDL-TG secretion, and increases fatty acid oxidation. This study demonstrates that although AADA is an additional carboxylester hydrolase besides TGH that resides within the ER, the functions of AADA and TGH in TG metabolism differ. In spite of earlier data implying a possible role for AADA in supporting VLDL assembly (28), our current results suggest that AADA functions as a negative regulator of VLDL assembly and cellular TG storage. It is yet unclear why the liver would harbor an ER-localized enzyme whose function would be to break down mainly newly synthesized DG, but it is possible that the enzyme has a role in futile cycling and diversion of fatty acids toward β-oxidation. Based on these results, AADA deserves further evaluation as a potential therapeutic target for combating hyperlipidemia and hepatic steatosis.

The authors thank Priscilla Gao for lipid analyses by gas chromatography, Johanne Lamoureux for technical assistance, and the members of the Lehner lab for comments during the study and for critical reading of this manuscript.

REFERENCES

1. Wiggins, D., and G. F. Gibbons. 1992. The lipolysis/esterification cycle of hepatic triacylglycerol. Its role in the secretion of very-low-density lipoprotein and its response to hormones and sulphonylureas. *Biochem. J.* **284:** 457–462.
2. Yang, L. Y., A. Kuksis, J. J. Myher, and G. Steiner. 1995. Origin of triacylglycerol moiety of plasma very low density lipoproteins in the rat: structural studies. *J. Lipid Res.* **36:** 125–136.
3. Lankester, D. L., A. M. Brown, and V. A. Zammit. 1998. Use of cytosolic triacylglycerol hydrolysis products and of exogenous fatty acid for the synthesis of triacylglycerol secreted by cultured rat hepatocytes. *J. Lipid Res.* **39:** 1889–1895.
4. Boren, J., S. Rustaeus, and S. O. Olofsson. 1994. Studies on the assembly of apolipoprotein B-100- and B-48-containing very low density lipoproteins in McA-RH7777 cells. *J. Biol. Chem.* **269:** 25879–25888.
5. Rustaeus, S., P. Stillemark, K. Lindberg, D. Gordon, and S. O. Olofsson. 1998. The microsomal triglyceride transfer protein catalyzes the post-translational assembly of apolipoprotein B-100 very low density lipoprotein in McA-RH7777 cells. *J. Biol. Chem.* **273:** 5196–5203.
6. Olofsson, S. O., P. Stillemark-Billton, and L. Asp. 2000. Intracellular assembly of VLDL: two major steps in separate cell compartments. *Trends Cardiovasc. Med.* **10:** 338–345.
7. Fisher, E. A., and H. N. Ginsberg. 2002. Complexity in the secretory pathway: the assembly and secretion of apolipoprotein B-containing lipoproteins. *J. Biol. Chem.* **277:** 17377–17380.
8. Yao, Z., and R. S. McLeod. 1994. Synthesis and secretion of hepatic apolipoprotein B-containing lipoproteins. *Biochim. Biophys. Acta.* **1212:** 152–166.
9. Mitchell, D. M., M. Zhou, R. Pariyarath, H. Wang, J. D. Aitchison, H. N. Ginsberg, and E. A. Fisher. 1998. Apoprotein B100 has a prolonged interaction with the translocon during which its lipidation and translocation change from dependence on the microsomal triglyceride transfer protein to independence. *Proc. Natl. Acad. Sci. USA.* **95:** 14733–14738.
10. Raabe, M., M. M. Veniant, M. A. Sullivan, C. H. Zlot, J. Bjorkegren, L. B. Nielsen, J. S. Wong, R. L. Hamilton, and S. G. Young. 1999. Analysis of the role of microsomal triglyceride transfer protein in the liver of tissue-specific knockout mice. *J. Clin. Invest.* **103:** 1287–1298.
11. Kulinski, A., S. Rustaeus, and J. E. Vance. 2002. Microsomal triacylglycerol transfer protein is required for lumenal accretion of

triacylglycerol not associated with ApoB, as well as for ApoB lipidation. *J. Biol. Chem.* **277:** 31516–31525.
12. Wang, Y., K. Tran, and Z. Yao. 1999. The activity of microsomal triglyceride transfer protein is essential for accumulation of triglyceride within microsomes in McA-RH7777 cells. A unified model for the assembly of very low density lipoproteins. *J. Biol. Chem.* **274:** 27793–27800.
13. Wang, H., D. Gilham, and R. Lehner. 2007. Proteomic and lipid characterization of apolipoprotein B-free luminal lipid droplets from mouse liver microsomes: implications for very low density lipoprotein assembly. *J. Biol. Chem.* **282:** 33218–33226.
14. Lehner, R., and D. E. Vance. 1999. Cloning and expression of a cDNA encoding a hepatic microsomal lipase that mobilizes stored triacylglycerol. *Biochem. J.* **343:** 1–10.
15. Gilham, D., S. Ho, M. Rasouli, P. Martres, D. E. Vance, and R. Lehner. 2003. Inhibitors of hepatic microsomal triacylglycerol hydrolase decrease very low density lipoprotein secretion. *FASEB J.* **17:** 1685–1687.
16. Gilham, D., M. Alam, W. Gao, D. E. Vance, and R. Lehner. 2005. Triacylglycerol hydrolase is localized to the endoplasmic reticulum by an unusual retrieval sequence where it participates in VLDL assembly without utilizing VLDL lipids as substrates. *Mol. Biol. Cell.* **16:** 984–996.
17. Dolinsky, V. W., D. N. Douglas, R. Lehner, and D. E. Vance. 2004. Regulation of the enzymes of hepatic microsomal triacylglycerol lipolysis and re-esterification by the glucocorticoid dexamethasone. *Biochem. J.* **378:** 967–974.
18. Gilham, D., and R. Lehner. 2004. The physiological role of triacylglycerol hydrolase in lipid metabolism. *Rev. Endocr. Metab. Disord.* **5:** 303–309.
19. Dolinsky, V. W., D. Gilham, M. Alam, D. E. Vance, and R. Lehner. 2004. Triacylglycerol hydrolase: role in intracellular lipid metabolism. *Cell. Mol. Life Sci.* **61:** 1633–1651.
20. Wei, E., M. Alam, F. Sun, L. B. Agellon, D. E. Vance, and R. Lehner. 2007. Apolipoprotein B and triacylglycerol secretion in human triacylglycerol hydrolase transgenic mice. *J. Lipid Res.* **48:** 2597–2606.
21. Coleman, R. A., E. B. Haynes, T. M. Sand, and R. A. Davis. 1988. Developmental coordinate expression of triacylglycerol and small molecular weight apoB synthesis and secretion by rat hepatocytes. *J. Lipid Res.* **29:** 33–42.
22. Lehner, R., Z. Cui, and D. E. Vance. 1999. Subcellullar localization, developmental expression and characterization of a liver triacylglycerol hydrolase. *Biochem. J.* **338:** 761–768.
23. Zimmermann, R., J. G. Strauss, G. Haemmerle, G. Schoiswohl, R. Birner-Gruenberger, M. Riederer, A. Lass, G. Neuberger, F. Eisenhaber, A. Hermetter, et al. 2004. Fat mobilization in adipose tissue is promoted by adipose triglyceride lipase. *Science.* **306:** 1383–1386.
24. Haemmerle, G., A. Lass, R. Zimmermann, G. Gorkiewicz, C. Meyer, J. Rozman, G. Heldmaier, R. Maier, C. Theussl, S. Eder, et al. 2006. Defective lipolysis and altered energy metabolism in mice lacking adipose triglyceride lipase. *Science.* **312:** 734–737.
25. Holm, C., T. Osterlund, H. Laurell, and J. A. Contreras. 2000. Molecular mechanisms regulating hormone-sensitive lipase and lipolysis. *Annu. Rev. Nutr.* **20:** 365–393.
26. Kraemer, F. B., and W. J. Shen. 2006. Hormone-sensitive lipase knockouts. *Nutr. Metab. (Lond).* **3:** 12.
27. Probst, M. R., M. Beer, D. Beer, P. Jeno, U. A. Meyer, and R. Gasser. 1994. Human liver arylacetamide deacetylase. Molecular cloning of a novel esterase involved in the metabolic activation of arylamine carcinogens with high sequence similarity to hormone-sensitive lipase. *J. Biol. Chem.* **269:** 21650–21656.
28. Trickett, J. I., D. D. Patel, B. L. Knight, E. D. Saggerson, G. F. Gibbons, and R. J. Pease. 2001. Characterization of the rodent genes for arylacetamide deacetylase, a putative microsomal lipase, and evidence for transcriptional regulation. *J. Biol. Chem.* **276:** 39522–39532.
29. Leung, D., C. Hardouin, D. L. Boger, and B. F. Cravatt. 2003. Discovering potent and selective reversible inhibitors of enzymes in complex proteomes. *Nat. Biotechnol.* **21:** 687–691.
30. Gilham, D., and R. Lehner. 2005. Techniques to measure lipase and esterase activity in vitro. *Methods.* **36:** 139–147.
31. Gilham, D., K. R. Perreault, C. F. Holmes, D. N. Brindley, D. E. Vance, and R. Lehner. 2005. Insulin, glucagon and fatty acid treatment of hepatocytes does not result in phosphorylation or changes in activity of triacylglycerol hydrolase. *Biochim. Biophys. Acta.* **1736:** 189–199.
32. Sahoo, D., T. C. Trischuk, T. Chan, V. A. Drover, S. Ho, G. Chimini, L. B. Agellon, R. Agnihotri, G. A. Francis, and R. Lehner. 2004. ABCA1-dependent lipid efflux to apolipoprotein A-I mediates HDL particle formation and decreases VLDL secretion from murine hepatocytes. *J. Lipid Res.* **45:** 1122–1131.
33. Folch, J., M. Lees, and G. H. Sloane Stanley. 1957. A simple method for the isolation and purification of total lipides from animal tissues. *J. Biol. Chem.* **226:** 497–509.
34. Hansson, P. K., A. K. Asztely, J. C. Clapham, and S. A. Schreyer. 2004. Glucose and fatty acid metabolism in McA-RH7777 hepatoma cells vs. rat primary hepatocytes: responsiveness to nutrient availability. *Biochim. Biophys. Acta.* **1684:** 54–62.
35. Tran, K., G. Thorne-Tjomsland, C. J. DeLong, Z. Cui, J. Shan, L. Burton, J. C. Jamieson, and Z. Yao. 2002. Intracellular assembly of very low density lipoproteins containing apolipoprotein B100 in rat hepatoma McA-RH7777 cells. *J. Biol. Chem.* **277:** 31187–31200.
36. Kraemer, F. B., S. Patel, M. S. Saedi, and C. Sztalryd. 1993. Detection of hormone-sensitive lipase in various tissues. I. Expression of an HSL/bacterial fusion protein and generation of anti-HSL antibodies. *J. Lipid Res.* **34:** 663–671.
37. Pease, R. J., D. Wiggins, E. D. Saggerson, J. Tree, and G. F. Gibbons. 1999. Metabolic characteristics of a human hepatoma cell line stably transfected with hormone-sensitive lipase. *Biochem. J.* **341:** 453–460.
38. Reid, B. N., G. P. Ables, O. A. Otlivanchik, G. Schoiswohl, R. Zechner, W. S. Blaner, I. J. Goldberg, R. F. Schwabe, S. C. Chua, Jr., and L. S. Huang. 2008. Hepatic overexpression of hormone-sensitive lipase and adipose triglyceride lipase promotes fatty acid oxidation, stimulates direct release of free fatty acids, and ameliorates steatosis. *J. Biol. Chem.* **283:** 13087–13099.
39. Lass, A., R. Zimmermann, G. Haemmerle, M. Riederer, G. Schoiswohl, M. Schweiger, P. Kienesberger, J. G. Strauss, G. Gorkiewicz, and R. Zechner. 2006. Adipose triglyceride lipase-mediated lipolysis of cellular fat stores is activated by CGI-58 and defective in Chanarin-Dorfman Syndrome. *Cell Metab.* **3:** 309–319.
40. Caviglia, J. M., J. D. Sparks, N. Toraskar, A. M. Brinker, T. C. Yin, J. L. Dixon, and D. L. Brasaemle. 2009. ABHD5/CGI-58 facilitates the assembly and secretion of apolipoprotein B lipoproteins by McA RH7777 rat hepatoma cells. *Biochim. Biophys. Acta.* **1791:** 198–205.
41. Brown, J. M., S. Chung, A. Das, G. Shelness, L. L. Rudel, and L. Yu. 2007. CGI-58 facilitates mobilization of cytoplasmic triglyceride for lipoprotein secretion in hepatoma cells. *J. Lipid Res.* **48:** 2295–2305.
42. Fredrikson, G., P. Stralfors, N. O. Nilsson, and P. Belfrage. 1981. Hormone-sensitive lipase of rat adipose tissue. Purification and some properties. *J. Biol. Chem.* **256:** 6311–6320.
43. Okazaki, H., M. Igarashi, M. Nishi, M. Sekiya, M. Tajima, S. Takase, M. Takanashi, K. Ohta, Y. Tamura, S. Okazaki, et al. 2008. Identification of neutral cholesterol ester hydrolase, a key enzyme removing cholesterol from macrophages. *J. Biol. Chem.* **283:** 33357–33364.
44. Hammond, L. E., P. A. Gallagher, S. Wang, S. Hiller, K. D. Kluckman, E. L. Posey-Marcos, N. Maeda, and R. A. Coleman. 2002. Mitochondrial glycerol-3-phosphate acyltransferase-deficient mice have reduced weight and liver triacylglycerol content and altered glycerolipid fatty acid composition. *Mol. Cell. Biol.* **22:** 8204–8214.
45. Vergnes, L., A. P. Beigneux, R. Davis, S. M. Watkins, S. G. Young, and K. Reue. 2006. Agpat6 deficiency causes subdermal lipodystrophy and resistance to obesity. *J. Lipid Res.* **47:** 745–754.
46. Reue, K., and P. Zhang. 2008. The lipin protein family: dual roles in lipid biosynthesis and gene expression. *FEBS Lett.* **582:** 90–96.
47. Coleman, R. A., and D. P. Lee. 2004. Enzymes of triacylglycerol synthesis and their regulation. *Prog. Lipid Res.* **43:** 134–176.
48. Nagle, C. A., L. Vergnes, H. Dejong, S. Wang, T. M. Lewin, K. Reue, and R. A. Coleman. 2008. Identification of a novel sn-glycerol-3-phosphate acyltransferase isoform, GPAT4, as the enzyme deficient in Agpat6−/− mice. *J. Lipid Res.* **49:** 823–831.
49. Donkor, J., M. Sariahmetoglu, J. Dewald, D. N. Brindley, and K. Reue. 2007. Three mammalian lipins act as phosphatidate phosphatases with distinct tissue expression patterns. *J. Biol. Chem.* **282:** 3450–3457.
50. Li, L. O., D. G. Mashek, J. An, S. D. Doughman, C. B. Newgard, and R. A. Coleman. 2006. Overexpression of rat long chain acyl-coa synthetase 1 alters fatty acid metabolism in rat primary hepatocytes. *J. Biol. Chem.* **281:** 37246–37255.